Molecular Cell, Vol. 13, 751–762, March 12, 2004, Copyright ©2004 by Cell Press

Snapshots of Replication through an Abasic Lesion: Structural Basis for Base Substitutions and Frameshifts

Hong Ling,[1,3] François Boudsocq,[2,4] Roger Woodgate,[2] and Wei Yang[1,*]
[1]Laboratory of Molecular Biology
National Institute of Diabetes and Digestive and Kidney Diseases
[2]Laboratory of Genomic Integrity
National Institute of Child Health and Human Development
National Institutes of Health
Bethesda, Maryland 20892

Summary

Dpo4 from *S. Solfataricus*, a DinB-like Y family polymerase, efficiently replicates DNA past an abasic lesion. We have determined crystal structures of Dpo4 complexed with five different abasic site-containing DNA substrates and find that translesion synthesis is template directed with the abasic site looped out and the incoming nucleotide is opposite the base 5′ to the lesion. The ensuing DNA synthesis generates a −1 frameshift when the abasic site remains extrahelical. Template realignment during primer extension is also observed, resulting in base substitutions or even +1 frameshifts. In the case of a +1 frameshift, the extra nucleotide is accommodated in the solvent-exposed minor groove. In addition, the structure of an unproductive Dpo4 ternary complex suggests that the flexible little finger domain facilitates DNA orientation and translocation during translesion synthesis.

Introduction

It is estimated that in a mammalian cell ~9000 bases are spontaneously lost each day, leaving behind apurinic and apyrimidinic (abasic) lesions (Nakamura et al., 1998). Although most abasic lesions are rapidly repaired via base excision repair pathways, a small number of remaining abasic sites impede DNA replication due to the lack of a template base to instruct nucleotide incorporation. To circumvent such replicative road blocks, cells often employ specialized DNA polymerases that are able to replicate through the damaged DNA (Goodman, 2002, Friedberg et al., 2002). Many translesion polymerases belong to the recently identified Y family of DNA polymerases (Ohmori et al., 2001), which are best characterized by their ability to synthesize DNA past a variety of lesions (translesion synthesis) and by their high error rate on undamaged templates (Woodgate, 1999; Goodman and Tippin, 2000; Kunkel and Bebenek, 2000; Goodman, 2002; Friedberg et al., 2002). The Y family polymerases Dpo4 (*D*NA *po*lymerase *IV*) and Dbh (*D*in*B* *h*omolog) from two related *Sulfolobus* strains are able to extend primer strands past abasic sites and in doing so generate predominantly −1 frameshift mutations (Potapova et al., 2002; Boudsocq et al., 2001; Kokoska et al., 2003).

Although sharing no detectable primary amino acid sequence homology with other replicative and repair polymerases, crystal structures of three Y family polymerases (archaeal Dpo4 and Dbh and *S. cerevisiae* Pol η) (Ling et al., 2001; Silvian et al., 2001; Trincao et al., 2001; Zhou et al., 2001) reveal a catalytic core consisting of thumb, finger, and conserved palm domains found in all DNA and RNA polymerases. The Y family polymerases also possess a unique C-terminal domain, called the little finger, wrist, or polymerase-associated domain (PAD) domain. The four domains fold into a half-open right-hand-like structure. The thumb and little finger domains contact the minor and major groove of DNA, respectively, holding the duplex portion of the DNA in the central cleft of the protein (Figure 1). A gap between the finger and little finger domains provides an entry channel for the single-stranded template. The palm domain contains the active site comprised of binding sites for the incoming nucleotide and divalent cations, and the finger domain interacts with the replicating base pair.

The two ternary-complex crystal structures of Dpo4 with undamaged DNA and an incoming nucleotide, referred to as type I (normal) and II (template misaligned), reveal a solvent accessible and spacious active site (Ling et al., 2001). The interactions between Dpo4 and the replicating base pair are limited to a few nonspecific van der Waals contacts, which provide a structural basis for its low fidelity and high error rate. In particular, the type II complex captures a template slippage (misalignment) toward the 5′ end such that Dpo4 avoids making a mismatched base pair by introducing a −1 frameshift (deletion) mutation. Similar slippage of Dpo4 on an undamaged DNA template has also been observed in solution (Kokoska et al., 2002).

The spacious and solvent-accessible active site of Dpo4 has recently been shown to accommodate *cis-syn* thymine dimers and benzo[*a*]pyrene hydrocarbon adducts (Ling et al., 2003, 2004). In those lesion-containing ternary complexes, the Dpo4 structure remains unchanged, and an incoming nucleotide still forms a base pair with the modified template in either a Watson-Crick or Hoogsteen configuration. In contrast, an abasic site is structurally different from the aforementioned bulky adducts, both of which retain at least some degree of coding information, in that the abasic site is truly noninstructional. How, then, does a polymerase incorporate a nucleotide opposite an abasic lesion?

Translesion synthesis usually encompasses two steps. The polymerase has to insert an incoming nucleotide opposite the lesion by catalyzing the nucleotidyl transfer reaction; subsequently, it has to extend the primer from the 3′ end opposite the lesion. Steric constraints or structural distortion due to DNA damage potentially impede both steps of DNA synthesis. The Dpo4 structures reported to date are snapshots of a single-

*Correspondence: wei.yang@nih.gov
[3]Present address: Department of Biochemistry, University of Western Ontario, London, Ontario N6A 5C1, Canada.
[4]Present address: Institut de Pharmacologie et de Biologie Structurale, CNRS, 31077 Toulouse, France.

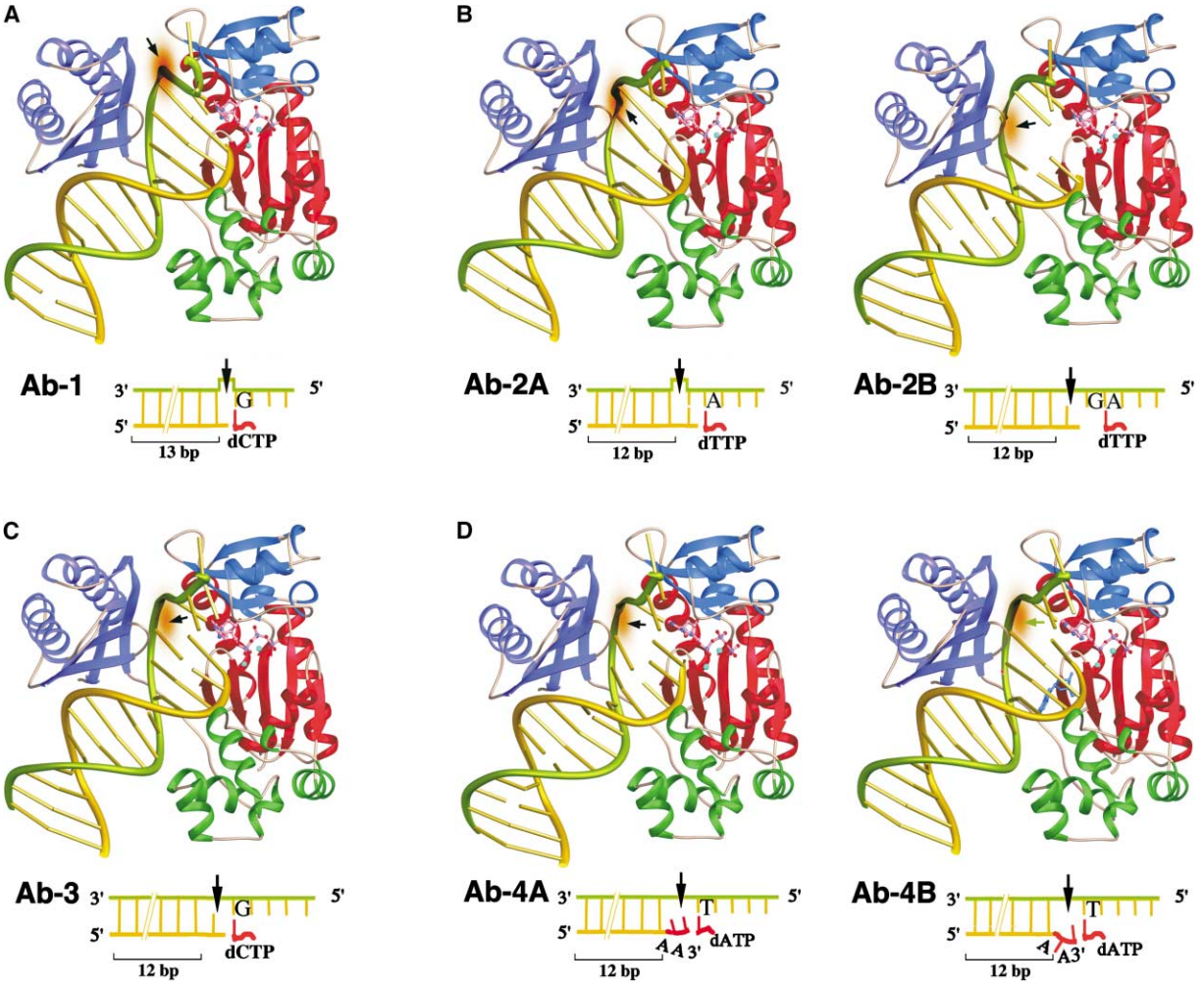

Figure 1. Abasic Lesion Bypass by Dpo4

(A) The Ab-1 complex. The base 5′ to the abasic lesion serves as a template, and the abasic site is looped out.

(B) The Ab-2A and Ab-2B complexes. Primer extension occurs with the abasic site remaining extrahelical (Ab-2A) or with DNA realignment (Ab-2B).

(C) The Ab-3 complex. Primer extension after template realignment. The abasic site is intrahelical opposite the dA at the 3′ end of the primer strand.

(D) The Ab-4A and Ab-4B complexes. Primer extension with a +1 frameshift. Two nucleotides of the primer strand are opposite the abasic lesion. In the 4A complex, all bases are intrahelical, and in the 4B complex, the second to the last nucleotide of the primer strand is flipped out and placed in the minor groove (shown in blue). The four domains of Dpo4 are shown as red (palm), green (thumb), blue (finger), and purple (little finger) ribbon diagrams, and the DNA as light green (template) and gold (primer) tubes. The incoming nucleoside triphosphate (pink bonds) is shown as a ball-and-stick model; the divalent metal ions in the active site as cyan spheres. The black arrow and orange brush indicate the site of an abasic lesion. A cartoon depicting the DNA structure surrounding the abasic site is given below each panel. Figures 1, 2, 3, 5, and 6 were made with Ribbons (Carson, 1987).

step that capture the polymerase either inserting a nucleotide opposite a damaged base (TT-1 and TT-2) (Ling et al., 2003) or extending a primer past a lesion site (BP-1 and BP-2) (Ling et al., 2004). We report here a series of crystal structures of Dpo4 inserting a nucleotide opposite an abasic lesion and subsequent primer extension past the lesion, which generate a base substitution, −1, or +1 frameshifts. In addition, we have also crystallized an unproductive ternary complex of Dpo4 with an abasic lesion, which reveals the inherit flexibility of Dpo4 that may enable it to bind and orient a DNA substrate for lesion accommodation and mutagenic DNA synthesis.

Results

Design of DNA Substrates and Crystal Structure Determination

To immobilize the DNA substrate and incoming nucleotide in a ternary complex with Dpo4 and to capture the abasic lesion at various desired positions relative to the Dpo4 active site, we used either an inactive 3′ dideoxy primer or replaced Mg^{2+} ions with Ca^{2+} during incubation prior to crystallization. Ca^{2+} greatly inhibits Dpo4's nucleotidyl transferase activity (our unpublished data). As reported in the previous crystal structures of Dpo4-DNA-nucleotide ternary complexes (Ling et al., 2001,

Table 1. Summary of Crystallographic Data

Crystal (Space Group)	Ab-1 ($P2_12_12$)	Ab-2 ($P2_12_12_1$)	Ab-3 ($P2_12_12$)	Ab-4 ($P2_12_12_1$)	Ab-5 ($P2_12_12_1$)
Unit cell (a, b, c) (Å)	99.1, 102.7, 53.2	98.3, 103.0, 105.4	98.4, 102.7, 52.3	98.0, 102.4, 105.7	75.5, 88.5, 92.4
Complexes per AU[a]	1	2	1	2	1
Nonhydrogen atoms[b]	3418 (23, 3)	7126 (376, 8)	3708 (338, 2)	7289 (526. 4)	3873 (389, 3)
Resolution range (Å)[c]	30–2.8 (2.85–2.80)	30–2.1 (2.14–2.10)	30–2.1 (2.14–2.10)	30–2.4 (2.44–2.40)	30–2.2 (2.24–2.20)
R_{merge}[c,d]	0.046 (0.378)	0.052 (0.404)	0.036 (0.252)	0.038 (0.399)	0.049 (0.239)
Unique reflections	12,345	61,046	30,778	39,503	29,643
Completeness (%)[c]	90.0 (81.0)	97.6 (95.3)	97.5 (95.3)	93.6 (80.0)	92.4 (60.1)
R value[e]	0.238	0.229	0.216	0.225	0.207
R_{free}[f]	0.275 (838 reflect.)	0.268 (1942 reflect.)	0.239 (915 reflect.)	0.263 (980 reflect.)	0.229 (981 reflect.)
Rmsd bond length (Å)	0.008	0.008	0.010	0.007	0.010
Rmsd bond angle (°)	1.31	1.54	1.67	1.27	1.75

[a] AU stands for asymmetric unit.
[b] The number of water molecules and divalent cations included in refinement is shown in parentheses separated by a comma.
[c] Data in the highest resolution shell are shown in parentheses.
[d] $R_{merge} = \Sigma_h\Sigma_i |I_{hi} - \langle I_h \rangle| / \Sigma \langle I_h \rangle$, where I_{hi} is the intensity of the ith observation of reflection h, and $\langle I_h \rangle$ is the average intensity of redundant measurements of the h reflections.
[e] R value $= \Sigma||F_o| - |F_c|| / \Sigma|F_o|$, where F_o and F_c are the observed and calculated structure-factor amplitudes.
[f] R_{free} is monitored with the reflections excluded from refinement in parentheses.

2003), the incoming nucleotide most often forms the fourteenth base pair of the DNA duplex within the crystal lattice. We chose to anneal an 18-mer template with an abasic site at either the fourteenth or thirteenth position from its 3′ end with a 13-mer primer to produce nucleotide insertion or primer extension complexes. Interestingly, the five Dpo4 ternary-complex structures reported here (Ab-1 to Ab-5) crystallized in three different lattices (Table 1), and the incoming nucleotide forms the thirteenth or fifteenth base pair in addition to the fourteenth. The 3′-dideoxy nucleotide of a primer strand was incorporated by Dpo4 using ddNTP (2′,3′-dideoxy nucleotide triphosphate) according to the template sequence (Ling et al., 2001). A specific incoming nucleotide was chosen based on the template sequence. When crystallizing an incoming nucleotide opposite the abasic site, we tried each of the four possible dNTPs and let Dpo4 determine the optimal substrate.

The new structures were determined by molecular replacement using the type I structure as a search model (Experimental Procedures). All five structures have been refined between 2.8 and 2.1 Å resolutions (Table 1). In all cases, the C-terminal 10–11 residues of Dpo4 are disordered as in type I and II structures (Ling et al., 2001). None of the protein residues are in the disallowed regions of Ramachandran plot.

Ab-1: Nucleotide Insertion Opposite an Abasic Lesion

The crystal structure of Ab-1 was obtained with an abasic site located at the fourteenth position from the 3′ end of the template and a 13-mer primer ending with a dG (Figure 1A). dATP, dGTP, dCTP, or dTTP was separately tried as the incoming nucleotide to crystallize a Dpo4 ternary complex in the presence of Ca^{2+}. Only with dCTP, which matched the template base 5′ to the abasic site (dG), did we obtain a diffraction-quality crystal of the ternary complex. The crystal was virtually isomorphous to the type I complex and diffracted X-rays to 2.8 Å resolution (Table 1). After refinement, we observe that the abasic site is looped out toward the solvent in the gap between the finger and little finger domains. The template dG 5′ to the abasic site and the incoming dCTP form a Watson-Crick base pair and stacks nicely with the preceding base pair in the DNA duplex. The 3′ end of the primer strand is 4.1 Å from the α-phosphate of dCTP (Figure 2A).

Ab-2: Primer Extension with a Single Nucleotide Deletion or −1 Frameshift

The crystal structure of Ab-2 was obtained in the presence of Ca^{2+} with an abasic site located at the thirteenth position from the 3′ end of the template, a 13-mer primer ending with a cytosine (dC) matching the template dG 5′ to the abasic site, and an incoming dTTP that paired with the next template base, dA (Figure 1B). The Ab-2 complex was crystallized in a different space group from Ab-1 (Table 1). There are two Dpo4 ternary complexes (A and B) in the asymmetric unit revealing two different conformations. The Ab-2 structure has been refined to 2.1 Å with R and R_{free} of 0.229 and 0.269, respectively. In the Ab-2A complex, the phosphate sugar backbone of the abasic site is bulged out as in Ab-1, and the thirteenth dC of the primer strand base pairs with the fourteenth dG (5′ to the abasic site) of the template strand (Figures 1B and 2B). The incoming dTTP is opposite the fifteenth dA and its α-phosphate is 4.1 Å from the 3′ end of the primer. In the Ab-2B complex, however, the primer strand is realigned so that the primer terminus is opposite the abasic site, the template dG next to the lesion has no partner, and the incoming dTTP is base-paired with dA two bases from the lesion (Figure 1B). The 3′-OH of the primer strand and the α-phosphate of dTTP are more than 6 Å apart. The Ab-2B complex resembles the type II Dpo4 structure, in which a template base is skipped over to avoid a mismatched base pair.

Ab-3: Primer Extension with Template Realignment and Generation of a Missense Mutation

Crystals of the Ab-3 complex were grown in the presence of Ca^{2+} with the abasic site located at the thirteenth position from the 3′ end of the template, a 13-mer primer with a dA at its 3′ end, and an incoming dCTP matching the template dG 5′ to the abasic site (Figure 1C). The

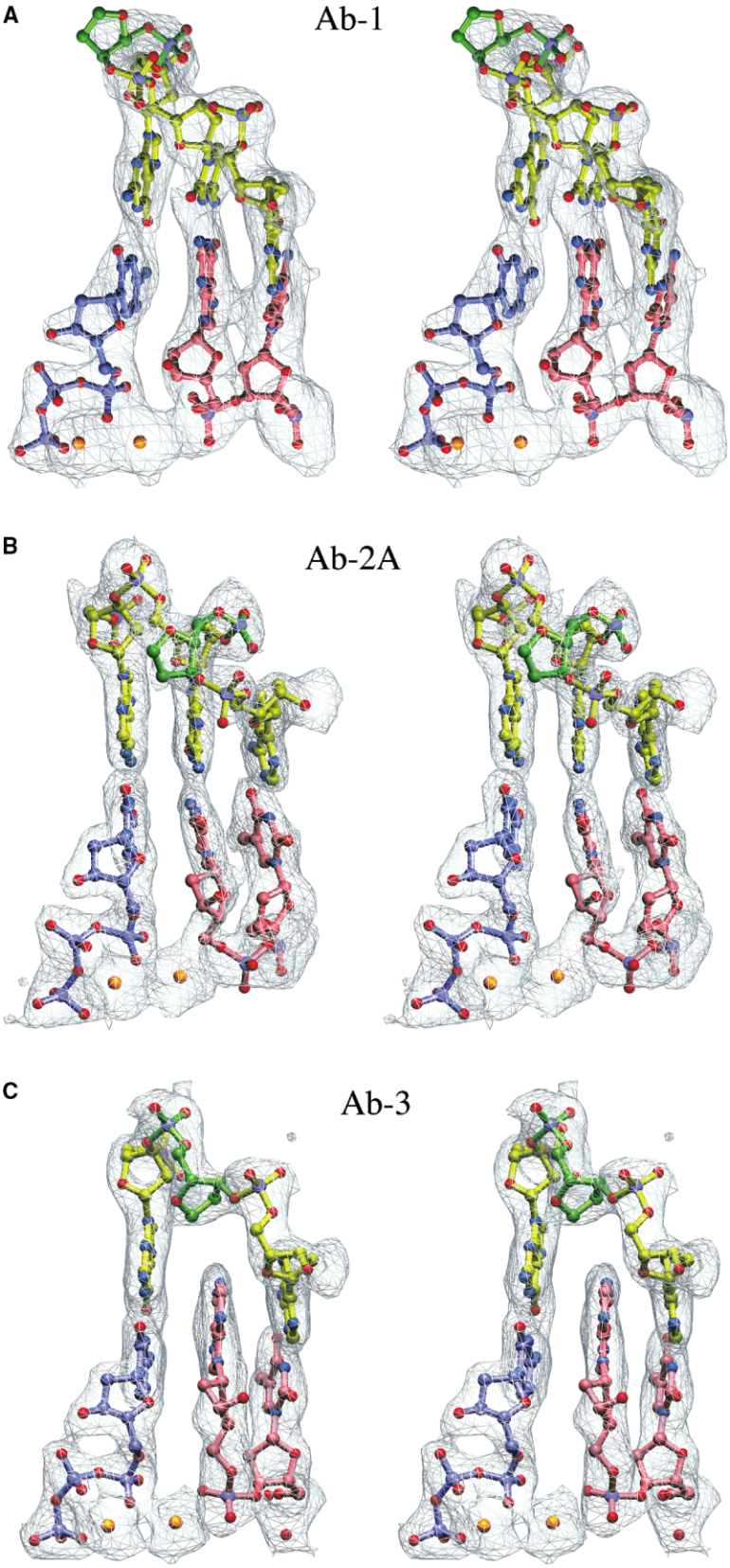

Figure 2. Close-Up Views of the Abasic Lesion in the Ab-1 (A), Ab-2A (B), and Ab-3 (C) Complexes

These structures represent the likely events when Dpo4 encounters an abasic lesion. Three base pairs including the incoming nucleotide and two metal ions are shown as ball-and-stick models and superimposed with a final refined $2F_o - F_c$ electron density map contoured at 1.0 σ (gray). The template strand is shown in yellow with the abasic site highlighted in green, the primer strand in pink, the incoming nucleotide in purple, and the divalent cations in orange.

Ab-3 crystal was isomorphous to the Ab-1 and diffracted X-rays to 2.1 Å resolution. The refined structure has an R and R_{free} of 0.216 and 0. 239, respectively. The 3′ dA of the primer is opposite the intrahelical abasic site, which is confirmed by the missing electron density for its base moiety. The incoming dCTP is opposite the template dG 5′ to the abasic site, and both the template and primer are in the correct base pair register. Because of the absence of a base at the lesion, the dA at the primer terminus slides toward the template strand and is stacked with the preceding bases of both strands (Figure 2C). The shift of the phosphosugar moiety of the dA leads to a larger separation (7 Å) between its 3′-OH and the α-phosphate of the incoming dCTP.

Ab-4: Primer Extension with a +1 Frameshift

The Ab-4 complex was generated when the abasic site was at the thirteenth position from the 3′ end of the template followed by a 5′ template dT, and the primer strand with a 3′-OH group was extended in the presence of dATP and Mg^{2+}. The primer strand initially contained 12 nucleotides but was extended to a 14-mer by Dpo4, and the incoming dATP was base-paired with the fourteenth dT of the template strand due to a +1 frameshift (Figure 1D). The Ab-4 crystal is isomorphous to that of Ab-2. Each asymmetric unit contains two Dpo4 ternary complexes (Ab-4A and Ab-4B) (Table 1). The first 12 bp are standard Watson-Crick type in both variations. In Ab-4A, the two additional dA (the thirteenth and fourteenth bases) of the primer strand are stacked within the duplex opposite the abasic lesion, but in Ab-4B the fourteenth base of the primer strand is opposite the abasic site, and the thirteenth base is flipped out of the DNA duplex and placed in the minor groove (Figures 1D, 3A, and 3B). Except for the extra base in the minor groove, the overall structure of the Ab-4B complex is very similar to that of Ab-3. In the Ab-4A complex the base insertion causes noticeable distortion in the DNA duplex. The 3′ dA of the primer strand is severely underwound (8° instead of 36°) and tilts toward the 5′ end, and the flanking twelfth base pair in the duplex is buckled toward the eleventh to accommodate the nucleotide insertion. Interestingly, the 3′-OH of the primer strand is still within 5 Å of the α-phosphate of dATP (Figure 3). In contrast, the 3′-OH and the α-phosphate of dATP in the Ab-4B structure are over 7 Å apart, similar to that in the Ab-3 structure. It is not clear which conformation of the Ab-4 complex is best suited for the nucleotidyl transfer reaction.

Solution Studies of Dpo4 Bypassing an Abasic Lesion

To verify the relevance of our Dpo4-abasic lesion complex structures, we analyzed abasic lesion bypass by Dpo4 using a radiolabeled 12-mer primer annealed to an abasic-containing 18-mer template. Four 18-mer templates with an abasic site at the thirteenth position followed by a different 5′ template base were tested (Figure 4). When all four dNTPs were provided, 94%–99% of the primer was extended by two or more bases, indicating that bypass of the abasic site was as robust as that observed with a longer DNA substrate (Boudsocq et al., 2001). In addition to the expected products, both −1 and +1 products (one nucleotide shorter or longer than the template) were observed in all cases. The −1 products were dominant when the abasic site was 3′ to a template dG, while the +1 products occurred when dT was 5′ to the lesion or on a normal template with two adjacent dTs (Figure 4). In the presence of a single dNTP, primers were extended most efficiently (80%–90%) when the incoming dNTP matched the base 5′ to the abasic site. The exception was when dA was 5′ to the lesion, where only 32% primers were extended using dTTP (Figure 4) compared to 55% with dATP. Interestingly, regardless of whether dG, dA, or dC was 5′ to the abasic lesion, ~50% of primers were extended by at least one nucleotide when dATP was supplied (Figure 4).

Ab-5: An Unproductive Complex

The preference for incorporating dA has been noted previously. When encountering a noninstructive lesion, such as abasic sites, DNA polymerases tend to incorporate dA by following the so-called "A rule" (Strauss, 1991). In an attempt to capture incorporation of dATP opposite an abasic lesion, an 18-mer template strand containing an abasic site at the fourteenth position from the 3′ end and a 13-mer primer with ddA at its 3′ end (added by Dpo4) were cocrystallized with Dpo4 and ddATP in the presence of Mg^{2+} and Ca^{2+}. To prevent template slippage stabilized by base pairing, dA instead of dT was placed 5′ to the abasic site in the template strand (Figure 5). In the resulting Ab-5 complex, however, the incoming ddATP was base-paired with the template dT 3′ to the abasic site instead of the abasic site itself, and the thirteenth nucleotide of the primer strand (ddA) is flipped into the minor groove (Figure 5A). The template strand makes a U turn at the abasic site and folds back toward the duplex portion of the DNA, and the Dpo4-substrate ternary complex is inactive.

Discussion

The 5′ Rule and −1 Frameshifts

−1 frameshift mutations have been well documented with the DinB-like polymerases in the presence of an abasic lesion. In addition to the Dpo4 data (Kokoska et al., 2002, 2003) (Figure 4), Dbh, a close relative of Dpo4, also tends to insert the nucleotide that forms a Watson-Crick pair with the base 5′ to the abasic site (Potapova et al., 2002), and the primer strand extended by Dbh or *E. coli* DinB is often one base shorter than the template (Potapova et al., 2002; Kobayashi et al., 2002). The −1 frameshift mutations are also made by Dbh, Dpo4, and *E.coli* DinB with normal DNA, and they occur most frequently at sites 3′ to a guanine (Kim et al., 1997; Wagner et al., 1999; Ohashi et al., 2000; Tang et al., 2000; Zhang et al., 2000; Kokoska et al., 2002). Our crystal structures show that Dpo4 does not utilize the abasic site to instruct nucleotide insertion. Dpo4 either takes a −1 frameshift approach to alleviate the lesion, as shown in the Ab-1 and Ab-2A structures, or becomes stalled if template misalignment is not feasible, as shown in the Ab-5 complex. Combined with the biochemical data, our crystal structures strongly suggest that in the presence of an abasic site, DinB homologs loop out the lesion and use

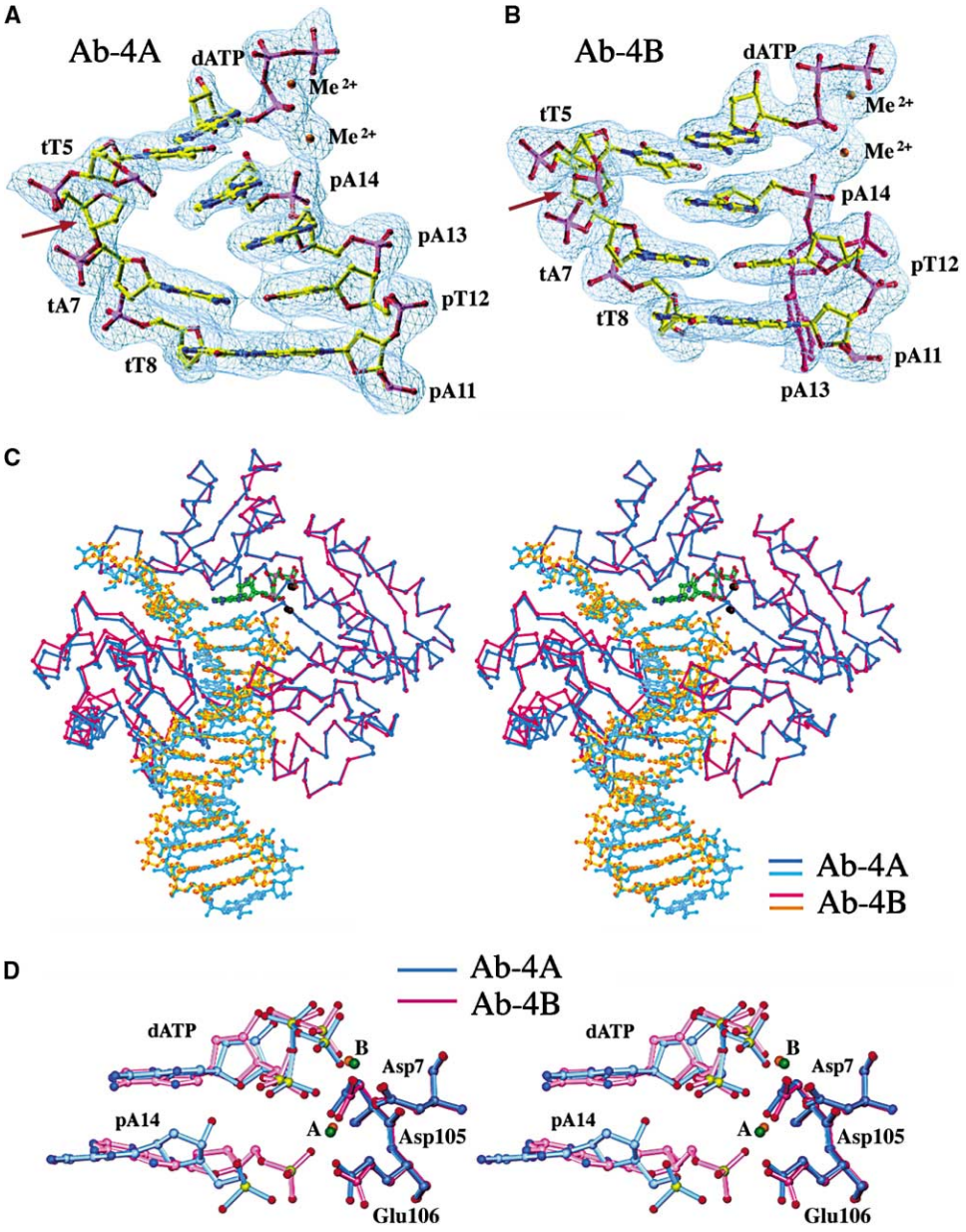

Figure 3. Correlation of the Movement of the Dpo4 Little Finger Domain and the DNA Orientation

(A and B) DNA structures surrounding the abasic site in the Ab-4A (A) and Ab-4B (B) complexes. A $2F_o - F_c$ map contoured at 1.0 σ is superimposed on the refined coordinates. The phosphorus atoms are shown in purple, oxygen in red, nitrogen in blue, and carbon in yellow. The divalent metal ions (Me^{2+}) are shown as orange balls. The backbone of the abasic site is marked by a red arrow. The extrahelical base in Ab-4B is highlighted in pink.

(C) Superposition of the Ab-4A and Ab-4B structures. Dpo4 is shown as Cα traces (Ab-4A in blue and Ab-4B in red), and DNA as stick models (Ab-4A in light blue and Ab-4B in yellow). The incoming nucleotides are in green, and the metal ions in dark brown.

(D) Comparison of the Dpo4 active site in the Ab-4A (blue) and Ab-4B (pink) structures. The three catalytic carboxylates, the metal ions (A and B), and the incoming nucleotide are approximately superimposable, but the 3′ terminal nucleotide of the primer strand is located differently. It is not clear which conformation is best suited for the nucleotidyl transfer reaction.

the base 5′ to the abasic site to instruct nucleotide incorporation, which we call the "5′ rule."

A −1 frameshift was first captured in the type II Dpo4-DNA complex when the polymerase skipped a template base to avoid a G:G mismatch and instead made a G:C base pair (Ling et al., 2001). However, the skipped dG template base was stacked within the DNA duplex rather than looped out, as in the Ab-1 and Ab-2A complexes. Indeed, it is impossible to keep the abasic site intrahelical while a −1 frameshift occurs at the lesion because the base pairs flanking the abasic lesion cannot form any base stacking without a base from either the template or primer strand. The −1 frameshift might also occur further away from the lesion, as shown in the Ab-2B complex, which is similar to the frameshift observed with undamaged DNA. Looping out of an abasic site near

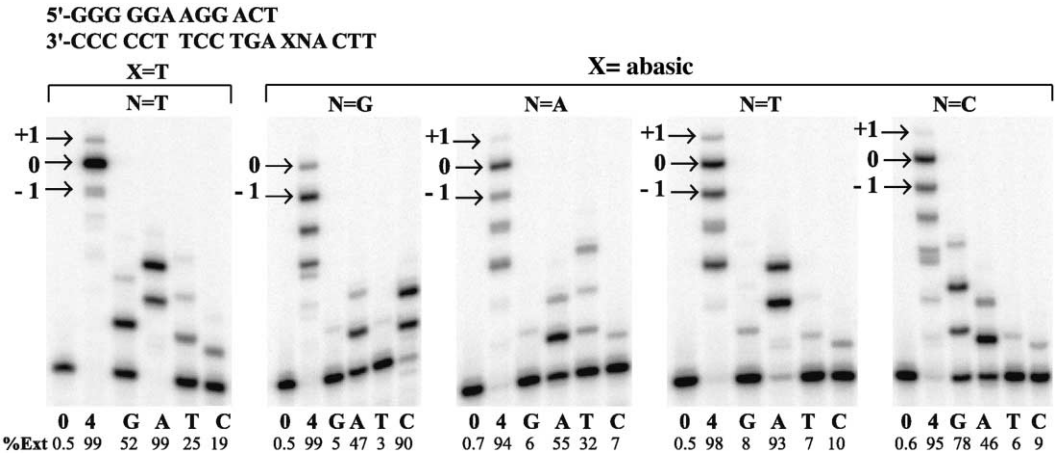

Figure 4. Nucleotide Incorporation Opposite an Abasic Site by Dpo4

The sequence of the primer/template is shown in the top left-hand corner, the local sequence context is given above each panel, and X represents the abasic site. The extent of nucleotide incorporation was measured with each template in the absence (0) or presence of all four nucleotides, or in the presence of each dNTP (100 μM G, A, T, or C). Reactions were carried out for 5 min at 37°C with 10 nM of Dpo4. The percentage of primer extension relative to the 0 dNTP control is given below each track. The arrows at the top left-hand side of each panel indicate the expected size of the full-length product (0), insertion (+1), or deletion (−1) products.

the active site, as in Ab-1 and Ab-2A, is probably only possible in the complexes of Dpo4 and related Y family polymerases due to the gap between the finger and little finger domains, which readily accommodates the abasic bulge in the template strand (Figure 1). In all crystal structures of replicative DNA polymerases, there is no such cavity to accommodate an abasic bulge next to the templating base. A replicative polymerase likely places an abasic lesion directly in the active site, which causes the polymerase to stall (Randall et al., 1987).

On the basis of the Ab-5 structure, we doubt that Dpo4 uses an abasic site to instruct incoming nucleotide selection. In fact, addition of dA to the primer strand may not require a template at all. For example, Dbh extends a blunt end DNA most efficiently with dATP (Potapova et al., 2002), and Dpo4 adds a dA to primer strands with the same efficiency regardless of the template sequence following the abasic lesion (Figure 4). The addition of dA at the 3′ end of DNA by the DinB-like polymerases may, therefore, be due to a nontemplated terminal nucleotidyl transferase activity rather than template-dependent polymerase activity. The high frequency of incorporation of dA opposite an abasic lesion in replication products may be partially explained by the ability of the Y family polymerases to extend the mismatched template primer as observed in the Ab-3 complex.

Template Realignment Leads to Base Substitutions and +1 Frameshifts

Replication products generated by Dpo4 or other DinB homologs are not exclusively single nucleotide deletions but are often the same length as the template strand even in the presence of abasic lesions (Figure 4) (Kokoska et al., 2003). This implies that, after the −1 misalignment that is required for nucleotide insertion, the template strand realigns during primer extension. DNA realignment is evident in the Ab-3 complex, in which the abasic site is in the correct register opposite the dA at the 3′ end of the primer strand (Figure 1C). Even though the Ab-2B structure appears abnormal (Figure 1B), the primer strand is clearly realigned. When dCTP, which supported the realignment with the correct register, instead of dTTP was provided, the Ab-3 structure was formed (Figure 1). Moreover, formation of the Ab-4 complexes can only be explained by DNA realignment (Figures 1D, 3A, and 3B). The two dAs incorporated into the primer strand by Dpo4 were probably both templated by the dT 5′ to the lesion. The first dA was likely incorporated with −1 misalignment as shown in the Ab-1 complex (the 5′ rule), and the second dA was incorporated after template realignment as shown in the Ab-3 structure. Such template realignment after misalignment readily explains base substitutions, particularly those in which the substitution is the same as the Watson-Crick pairing partner of the 5′ template base (Kokoska et al., 2002, 2003).

As a result of primer extension without template translocation, the Ab-4 complex represents a +1 frameshift with two dAs opposite a single abasic site. It is curious, however, that even in the presence of Mg^{2+} the nucleotidyl transfer reaction is not observed in the Ab-4 complex even though the incoming dATP is base-paired with the dT 5′ to the lesion. The absence of a +1 frameshift product in the crystal structure may be explained by (1) the low efficiency of the reaction and incomplete conversion of the primer strands and (2) the lack of an appropriate incoming nucleotide (dTTP) to stabilize the +1 frameshift product in a Dpo4 ternary complex. We have so far been unable to crystallize a Dpo4 binary complex without an incoming nucleotide. It is likely that in the crystallization drop both species of the primer strand, extended by a +1 frameshift mechanism as well as nonextended, were present, but only the nonextended species was crystallized since it was favored by the presence of dATP.

Frameshifts due to nucleotide insertions are rarely

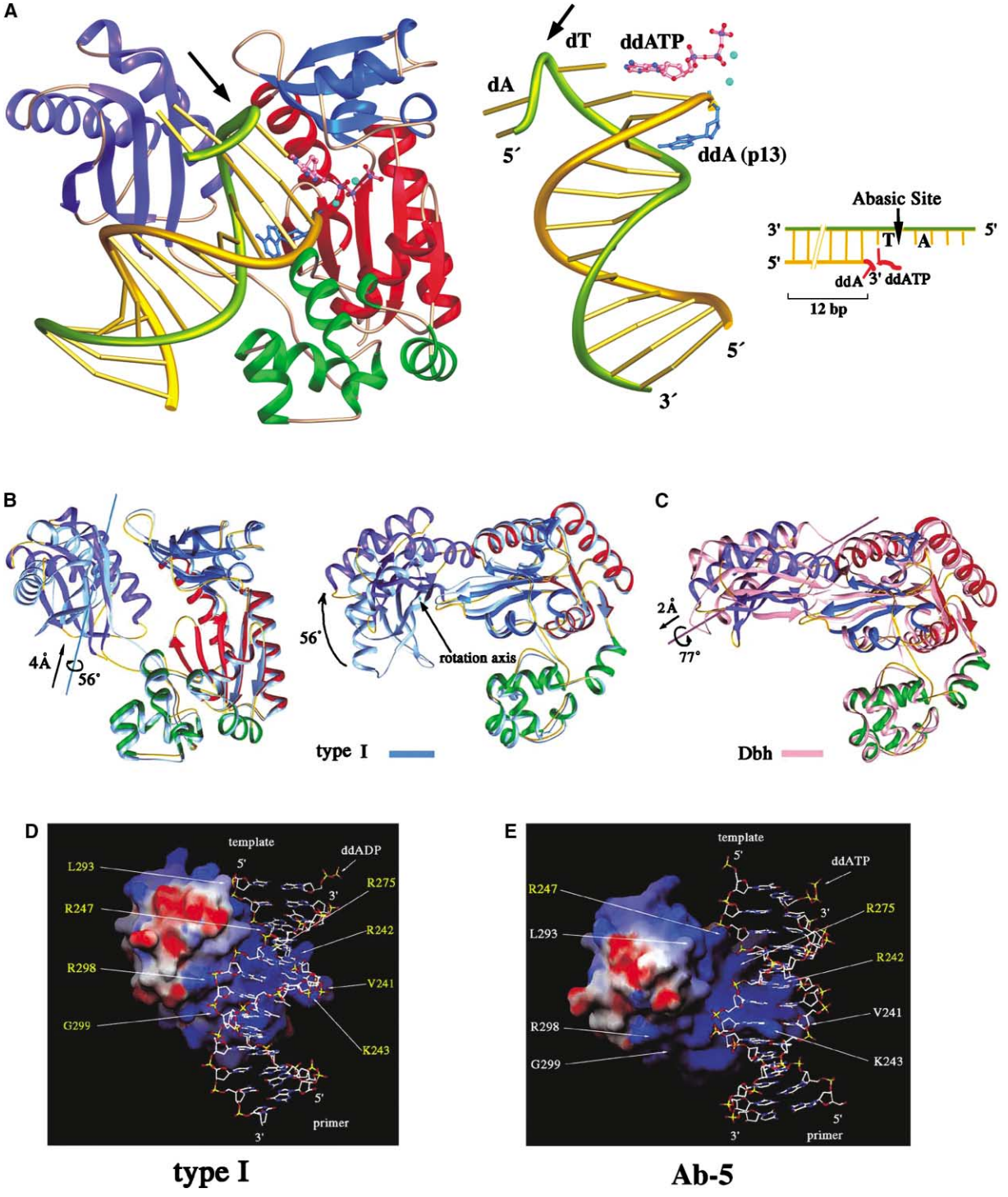

Figure 5. An Unproductive Dpo4 Ternary Complex and the Movement of the Little Finger Domain

(A) The Ab-5 complex. ddA at the 3′ end of the primer, which should be base-paired with the template base 3′ to the abasic lesion, is flipped out into the minor groove, and the incoming ddATP takes its place. The color scheme for the figure is the same as that used in Figure 1.

(B) Rigid-body movement of the little finger domain. Orthogonal views of the superimposition of the type I and Ab-5 Dpo4 structures. The Ab-5 structure is shown in the same color scheme as in Figure 1, and the type I in light blue. The three domains in the catalytic core are virtually the same, but the little finger domain is rotated and translated along the axis depicted in blue.

(C) Superimposition of the Dpo4 (Ab-5) and Dbh (in pink) (Silvian et al., 2001) displayed in the same orientation as in (B). The location of the Dbh little finger relative to that of Dpo4 is indicated.

(D and E) Interactions between the little finger domain and DNA in the type I and Ab-5 complexes. The little finger domain is depicted by molecular surface where blue and red represent positive and negative electrostatic potentials. The duplex portion of DNA including the incoming nucleotide is shown as stick models. Protein residues in close contact with DNA are labeled in yellow. In the Ab-5 complex, the little finger moves away from the major groove and makes very few contacts with DNA. (D) and (E) were made with graphic program GRASP (Nicholls et al., 1991).

detected in the mutational spectra of DNA synthesis through abasic lesions by Dpo4 (Kokoska et al., 2003), which raises the question of the physiological relevance of a +1 frameshift. It is possible that the +1 products observed with Dpo4 (Figure 4) may be due to the terminal nucleotide transferase activity of DinB-like polymerases (Ling et al., 2004; Potapova et al., 2002). In the case of Dpo4, the amount of +1 products generated is DNA sequence dependent and is most abundant when the abasic lesion is followed by a 5′ dT (Figure 4), but the DNA sequence in the middle of a template strand should have no effect if the insertions were the result of terminal transferase activity. We suspect that +1 frameshifts do occur in solution as depicted in the Ab-4 crystal, but only on short templates, which probably suppress template translocation. When a longer abasic DNA substrate is utilized, the amount of the +1 product is greatly reduced, and there is a concomitant increase of −1 events, both at 37°C and 60°C (F.B., unpublished data). The latter observation agrees well with data obtained with other DinB homologs (Potapova et al., 2002; Kobayashi et al., 2002). The Ab-4 structures nevertheless demonstrate that a +1 frameshift mutation, however rare, is possible.

A Rigid Catalytic Core

The Dpo4 structures in the Ab-1 to Ab-4 complexes are essentially identical to those that are complexed with normal DNA, a thymine dimer and a benzo[*a*]pyrene adduct (Ling et al., 2001, 2003, 2004). The root-mean-square deviations (rmsd) over all 341 Cα atoms of Dpo4 range from 0.3 to 0.6 Å after pairwise superposition of these structures. The catalytic core, consisting of palm, finger, and thumb domains, remains structurally constant among these Dpo4-DNA cocrystals (rmsd under 0.4 Å) (Figure 3C).

Among the Ab-1, Ab-2, Ab-3, and Ab-4 complexes, the organization of the active site, which includes the three carboxylates (Asp7, Asp105, and Glu106), two metal ions, the 3′-OH of the primer strand, and an incoming nucleotide, are comparable with those observed in T7 and Taq DNA polymerases (Doublie et al., 1998; Li et al., 1998) (Figure 3D), suggesting that the catalytic mechanism of nucleotidyl transfer reaction is conserved in these polymerases. The carboxylates are superimposable in all cases. One metal ion that is equivalent to metal B in the T7 and Taq polymerases is coordinated with nearly ideal octahedral geometry by the carboxylates of Asp7 and Asp105, and the α-, β-, and γ-phosphates of the incoming nucleotide (Figure 3D). The other metal ion (A site), which mediates the interaction between the primer strand, the α-phosphate of dNTP, and the catalytic carboxylates, is less well defined than the B site. Since the 3′-OH of the primer is at least 4 Å away from the α-phosphate of an incoming nucleotide in the Dpo4 structures solved to date, the coordination of the A site metal does not represent the active form. This could be a result of Ca^{2+} replacement of Mg^{2+}, but it could also reflect the relative low catalytic efficiency of the polymerase.

As noted previously (Ling et al., 2003), the catalytic cores of Dpo4 and Dbh are superimposable despite the fact that Dpo4 was crystallized with a DNA substrate and Dbh in the absence of DNA. The rms deviation in the catalytic core between the two proteins is 0.9 Å over 187 pairs of Cα atoms (PDB: 1VAS) or 1.35 Å over 229 pairs of Cα atoms (PDB: 1K1Q) (Figure 5C). The main differences between the catalytic cores of the two proteins are that the thumb domain is slightly reoriented (< 0.5 Å) relative to the palm and finger domain and the solvent exposed loop regions in the finger domain undergo some conformational changes. In contrast, the finger domain of DNA polymerases in the A, B, and X families undergoes dramatic conformational changes upon binding of a corrrect incoming nucleotide (Franklin et al., 2001; Johnson et al., 2003; Li et al., 1998; Pelletier et al., 1996). This difference suggests that Dbh and Dpo4 do not perform conformation-dependent fidelity check (Zhou et al., 2001).

The Flexible Little Finger Domain Facilitates DNA Orientation and Translocation

The little finger domain, which is unique to the Y family polymerases, is mobile and can be cleaved off from the catalytic core in the absence of DNA by trypsin digestion (Ling et al., 2001). The little finger alone is superimposable among all Dpo4 structures with an rmsd of 0.35 Å, but in the Ab-5 complex, it rotates 56° and translates 4 Å as a rigid body toward the finger domain closing the gap between the two domains (Figure 5B). Concomitantly, the single-stranded template, which used to be held in the gap, now makes a U turn at the abasic site and becomes solvent exposed (Figure 5A). The movement of the little finger domain in Ab-5 also exposes the DNA major groove and reduces the contact surface between Dpo4 and DNA from 940 ± 20 $Å^2$ to 748 $Å^2$ (Figures 5D and 5E). The DNA duplex near the active site is shifted away from Dpo4 by ~2 Å, and the other end of the duplex, which has no specific contacts with Dpo4, deviates even more.

Displacement of the little finger domain renders the Ab-5 structure very different from all other Dpo4 ternary complexes, but reminiscent of the Dbh apoprotein structure (Figure 5C). We suspect that the Ab-5 complex represents a structural intermediate between apoprotein and an active ternary complex and that the flexible little finger domain probably supports DNA translocation. The little finger domain has also been suggested to increase the catalytic efficiency of Dpo4 by stabilizing the bound DNA substrate (Ling et al., 2001). Comparison of the type I and Ab-1 to Ab-4 structures reveals that the movement of the little finger domain is correlated with the orientation of the DNA substrate relative to the catalytic core (Figure 3C), suggesting that the mobile little finger domain may facilitate the DNA substrate alignment and orientation for catalysis. Interestingly, the little finger domain is the least conserved among Y family polymerases. This variable domain may influence both the catalytic efficiency and substrate (lesion) preference of each Y family polymerase.

DNA Distortion and Implications for Bypassing Bulky DNA Adducts

The Ab-1, Ab-2A, Ab-4B, and Ab-5 structures contain DNA bulges (loop out) in either the template or primer strand. The abasic bulge of the template strand in the Ab-1 and Ab-2A complexes is readily accommodated

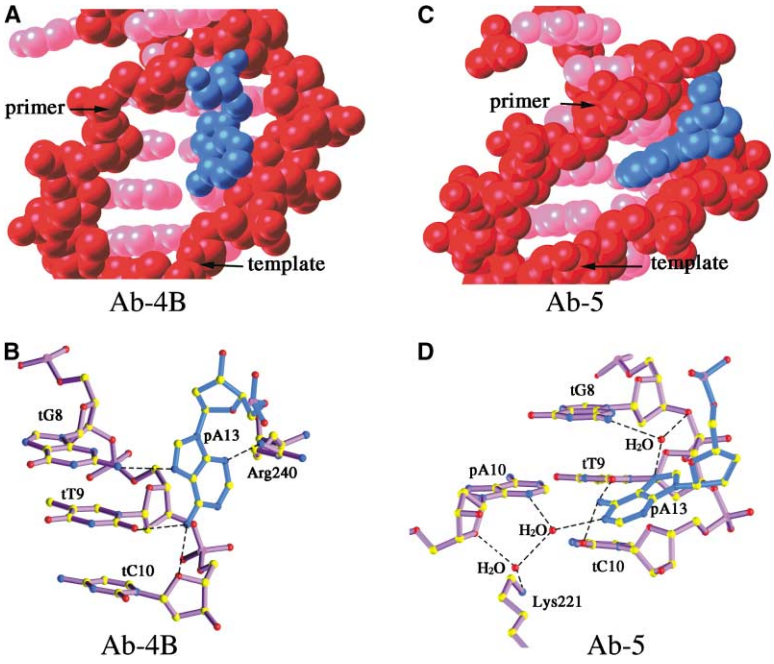

Figure 6. An Extrahelical Base in the Minor Groove

(A and B) The inserted base (in dark blue) in the type Ab-4B complex is stacked with the template strand (in red and pink).

(C and D) The inserted base in the Ab-5 complex is sandwiched between the primer and template strands. Hydrogen bonds, which stabilize the extrahelical base, are shown in (B) and (D).

in the gap between the finger and little finger domains of Dpo4, and the base pairs surrounding the bulge remain normal B form in both cases. In the Ab-4B and Ab-5 structures, the extrahelical base from the primer strand is inserted into the DNA minor groove (Figure 6), a conformation which has not been observed previously in structures of DNA alone or protein-DNA complexes. Extrahelical bases have been observed in DNA complexes with DNA glycosylase or methyltranferase, but the flipped-out base is inserted into the protein active site as a substrate (Barrett et al., 1999; Fromme and Verdine, 2002; Lau et al., 1998; Parikh et al., 2000; Roberts and Cheng, 1998). The extrahelical bases in the Ab-4B and Ab-5 complexes, however, interact mostly with DNA. Only one protein residue, Arg240 in Ab-4B and Lys221 in Ab-5, is involved in hydrogen bonding with the flipped-out base. Insertion into the minor groove is possible because of the relatively small finger and thumb domains of Dpo4, which leave the minor groove near the active site solvent accessible (Ling et al., 2001). The base pairs equivalent to those that are involved in hydrogen bonding with the extrahelical bases in the Dpo4 complexes (−3 to −4 from the replication base pair) (Figure 6) are surrounded by protein residues when complexed with the high-fidelity A and B family polymerases. Only Watson-Crick base pairs with a smooth minor groove can be accommodated at these positions in the replicative DNA polymerase complexes (Li et al., 1998; Doublie et al., 1999).

The extrahelical base is stacked against the template strand in the Ab-4B complex (Figures 6A and 6B) but sandwiched between the DNA backbones narrowing the minor groove from 8 Å to ~5 Å in the Ab-5 complex (Figures 6C and 6D). The different hydrogen bond networks surrounding the extrahelical base in the Ab-4B and Ab-5 complexes suggest that the minor groove may accommodate other bases or large hydrocarbon adducts. The dG-N^2-BPDE (*b*enzo[*a*]pyrene *d*iol *e*poxide) adduct, which blocks DNA replication by A and B family polymerases but is readily bypassed by DinB-like polymerases (Shen et al., 2002; Zhang et al., 2000; Rechkoblit et al., 2002; Suzuki et al., 2002), is located in the DNA minor groove (Cosman et al., 1992) and may thus be accommodated in a similar manner during translesion synthesis.

Conclusions

Our crystal structures of Dpo4 complexed with abasic lesions suggest that the insertion step of translesion synthesis is template dependent, with the base 5′ to the lesion instructing nucleotide incorporation, while the lesion itself is bulged out. During primer extension, the abasic bulge may be retained and replication products thus contain a single nucleotide deletion. Alternatively, the template strand may realign during primer extension and lead to a base substitution mutation. The relatively rigid catalytic core of Dpo4 and Dbh, particularly the palm and finger domains, indicates that the DinB branch of the Y family polymerases do not undergo a discernable nucleotide-induced conformation change in the finger domain, a process often observed in the high-fidelity DNA polymerases and known as "induced fit" (Doublie et al., 1999; Wong et al., 1991). Instead, the little finger domain undergoes rigid body movement that depends upon the DNA substrate and the base-pairing potential between the incoming nucleotide and template strand. Such movement probably facilitates the accommodation of a distorted DNA template for translesion synthesis and enables DNA translocation between successive rounds of nucleotidyl transfer.

Experimental Procedures

Sample Preparation and Crystallization

Full-length Dpo4 was overexpressed and purified as described (Boudsocq et al., 2001; Ling et al., 2001). The integrity of the protein was confirmed by mass spectrometry. The protein was concen-

trated to 15 mg/ml in a buffer containing 100 mM NaCl and 20 mM HEPES (pH 7.0). Purified oligonucleotides were purchased from Oligos Etc. Inc. An 18 nt template containing an abasic analog, tetrahydrofuran, at either the thirteenth or fourteenth position from the 3′ end (Ab-1, 5′-TACGXCGTGATCAGTGCC-3′; Ab-2 5′-TTCA GXAGTCCTTCCCCC-3′; Ab-3, 5′-TTCAGXAGTCCTTCCCCC-3′; Ab-4, 5′-TTCATXAGTCCTTCCCCC-3′; Ab-5, 5′-TTCAXTAGTCCTTCCCCC-3′) and a complementary 12 or 13 base primer (Ab-1, 5′-GGCACTGAT CACG-3′; Ab-2, 5′-GGGGGAAGGACTC-3′; Ab-3, 5′-GGGGGAAG GACTA-3′; Ab-4 and Ab-5, 5′-GGGGGAAGGACT-3′) were annealed and mixed with Dpo4 in 1.2:1 molar ratio. The protein-DNA complexes were concentrated using a centricon filter to a final protein concentration of ~8 mg/ml. The protein-DNA complexes were then incubated with an appropriate incoming nucleotide at 1 mM concentration in the presence of Mg^{2+} or Ca^{2+}. dCTP and 5 mM $CaCl_2$ were used to produce the Ab-1 and Ab-3 crystals, $CaCl_2$ and dTTP for the Ab-2 crystals, dATP and $MgCl_2$ for the Ab-4 crystals, and $MgCl_2$ and ddATP for the Ab-5 crystals. The crystals were produced by the hanging drop method against a reservoir solution containing 100 mM HEPES 7.0, 100 mM calcium acetate, 12%–15% PEG 3350, and 2% glycerol at 20°C. Crystals were transferred to a cryosolution containing the mother liquor with 25% PEG 3350 and 15% ethylene glycol and flash frozen in liquid propane.

Structure Determination and Refinement

Diffraction data of the five crystal forms were collected at −178°C with an R axis IPII detector mounted on a Rigaku RU 200 generator. The data were processed using DENZO and SCALEPACK (Otwinowski and Minor, 1997). The structures were determined by molecular replacement using CNS 1.0 (Brünger et al., 1998) and the type I structure as a search model (Ling et al., 2001). The models were refined with manual adjustment using O and CNS (Jones et al., 1991; Brünger et al., 1998). Noncrytallographic symmetry restraints was applied to the refinement of the Ab-4 structure.

In Vitro Translesion Replication Reactions

Oligonucleotides used in the replication assays were synthesized by Lofstrand Laboratories (Gaithersburg, MD) and gel purified prior to use. Templates were 18-mers containing a uniquely placed synthetic abasic site, indicated by an X. In each case, the template base 5′ to the abasic site was either A, T, G, or C. The 18-mer templates were FBHL18AB13G (5′-TTCAGXAGTCCTTCCCCC-3′); FBHL18AB13C (5′-TTCACXAGTCCTTCCCCC-3′), FBHL18AB13A (5′-TTCAAXAGTCCTTCCCCC-3′), and FBHL18AB13T (5′-TTCAT XAGTCCTTCCCCC-3′). All were primed with a 12-mer (FBHL12T) (5′-GGGGGAAGGACT-3′) that was 5′ labeled with [α-^{32}P]ATP (5000 Ci/mmole; 1 Ci = 37 GBq) (Amersham-Pharmacia) using T4 polynucleotide kinase. The primer and each abasic-containing unlabeled template were annealed at a molar ratio of 1:1.5.

Standard 10 μl reactions contained 40 mM Tris-HCl at pH 8.0, 5 mM $MgCl_2$, 100 μM of each ultrapure dNTPs (Amersham Pharmacia Biotech, NJ), 10 mM DTT, 250 μg/ml BSA, 2.5% glycerol, 20–30 nM 5′ [^{32}P] primer-template DNA and 10 nM Dpo4. After incubation at 37°C for 5 min, reactions were terminated by the addition of 10 μl of 95% formamide/10 mM EDTA and the samples heated to 100°C for 5 min. Reaction mixtures (5 μl) were subjected to 20% polyacrylamide/7 M Urea gel electrophoresis and replication products were visualized by PhosphorImager analysis.

Acknowledgments

We thank Drs. R. Craigie and D. Leahy for critical reading of the manuscript and the referees for insightful comments.

Received: November 25, 2003
Revised: January 13, 2004
Accepted: January 22, 2004
Published: March 11, 2004

References

Barrett, T.E., Scharer, O.D., Savva, R., Brown, T., Jiricny, J., Verdine, G.L., and Pearl, L.H. (1999). Crystal structure of a thwarted mismatch glycosylase DNA repair complex. EMBO J. *18*, 6599–6609.

Boudsocq, F., Iwai, S., Hanaoka, F., and Woodgate, R. (2001). Sulfolobus solfataricus P2 DNA polymerase IV (Dpo4): an archaeal DinB-like DNA polymerase with lesion-bypass properties akin to eukaryotic Pol η. Nucleic Acids Res. *29*, 4607–4616.

Brünger, A.T., Adams, P.D., Clore, G.M., Delane, W.L., Gros, P., Grosse-Kunstleve, R.W., Jiang, J.-S., Kuszewski, J., Nilges, M., Pannu, N. S., et al. (1998). Crystallography and NMR system: a new software suite for macromolecular structure determination. Acta Crystallogr. D *54*, 905–921.

Carson, M. (1987). Ribbon models of macromolecules. J. Mol. Graph. *5*, 103–106.

Cosman, M., de los Santos, C., Fiala, R., Hingerty, B.E., Singh, S.B., Ibanez, V., Margulis, L.A., Live, D., Geacintov, N.E., Broyde, S., et al. (1992). Solution conformation of the major adduct between the carcinogen (+)-anti-benzo[*a*]pyrene diol epoxide and DNA. Proc. Natl. Acad. Sci. USA *89*, 1914–1918.

Doublie, S., Tabor, S., Long, A.M., Richardson, C.C., and Ellenberger, T. (1998). Crystal structure of a bacteriophage T7 DNA replication complex at 2.2 Å resolution. Nature *391*, 251–258.

Doublie, S., Sawaya, M.R., and Ellenberger, T. (1999). An open and closed case for all polymerases. Structure Fold. Des. *7*, R31–R35.

Franklin, M.C., Wang, J., and Steitz, T.A. (2001). Structure of the replicating complex of a Pol α family DNA polymerase. Cell *105*, 657–667.

Friedberg, E.C., Wagner, R., and Radman, M. (2002). Specialized DNA polymerases, cellular survival, and the genesis of mutations. Science *296*, 1627–1630.

Fromme, J.C., and Verdine, G.L. (2002). Structural insights into lesion recognition and repair by the bacterial 8-oxoguanine DNA glycosylase MutM. Nat. Struct. Biol. *9*, 544–552.

Goodman, M.F. (2002). Error-prone repair DNA polymerases in prokaryotes and eukaryotes. Annu. Rev. Biochem. *71*, 17–50.

Goodman, M.F., and Tippin, B. (2000). The expanding polymerase universe. Nat. Rev. Mol. Cell Biol. *1*, 101–109.

Johnson, S.J., Taylor, J.S., and Beese, L.S. (2003). Processive DNA synthesis observed in a polymerase crystal suggests a mechanism for the prevention of frameshift mutations. Proc. Natl. Acad. Sci. USA *100*, 3895–3900.

Jones, T.A., Zou, J.-Y., and Cowan, S.W. (1991). Improved methods for building models in electron density maps and the location of errors in these models. Acta Crystallogr. A *47*, 110–119.

Kim, S.R., Maenhaut-Michel, G., Yamada, M., Yamamoto, Y., Matsui, K., Sofuni, T., Nohmi, T., and Ohmori, H. (1997). Multiple pathways for SOS-induced mutagenesis in *Escherichia coli*: an overexpression of dinB/dinP results in strongly enhancing mutagenesis in the absence of any exogenous treatment to damage DNA. Proc. Natl. Acad. Sci. USA *94*, 13792–13797.

Kobayashi, S., Valentine, M.R., Pham, P., O'Donnell, M., and Goodman, M.F. (2002). Fidelity of *Escherichia coli* DNA polymerase IV. Preferential generation of small deletion mutations by dNTP-stabilized misalignment. J. Biol. Chem. *277*, 34198–34207.

Kokoska, R.J., Bebenek, K., Boudsocq, F., Woodgate, R., and Kunkel, T.A. (2002). Low fidelity DNA synthesis by a Y family DNA polymerase due to misalignment in the active site. J. Biol. Chem. *277*, 19633–19638.

Kokoska, R.J., McCulloch, S.D., and Kunkel, T.A. (2003). The efficiency and specificity of apurinic/apyrimidinic site bypass by human DNA polymerase η and *Sulfolobus solfataricus* Dpo4. J. Biol. Chem. *278*, 50537–50545.

Kunkel, T.A., and Bebenek, K. (2000). DNA replication fidelity. Annu. Rev. Biochem. *69*, 497–529.

Lau, A.Y., Scharer, O.D., Samson, L., Verdine, G.L., and Ellenberger, T. (1998). Crystal structure of a human alkylbase-DNA repair enzyme complexed to DNA: mechanisms for nucleotide flipping and base excision. Cell *95*, 249–258.

Li, Y., Korolev, S., and Waksman, G. (1998). Crystal structures of open and closed forms of binary and ternary complexes of the large fragment of Thermus aquaticus DNA polymerase I: structural basis for nucleotide incorporation. EMBO J. *17*, 7514–7525.

Ling, H., Boudsocq, F., Woodgate, R., and Yang, W. (2001). Crystal structure of a Y-family DNA polymerase in action: a mechanism for error-prone and lesion-bypass replication. Cell *107*, 91–102.

Ling, H., Boudsocq, F., Plosky, B.S., Woodgate, R., and Yang, W. (2003). Replication of a cis-syn thymine dimer at atomic resolution. Nature *424*, 1083–1087.

Ling, H., Sayer, J.M., Plosky, B.S., Yagi, H., Boudsocq, F., Woodgate, R., Jerina, D.M., and Yang, W. (2004). Crystal structure of a Benzo[*a*]-pyrene diol epoxide adduct in a ternary complex with a DNA polymerase. Proc. Natl. Acad. Sci. USA, *101*, 2265–2269.

Nakamura, J., Walker, V.E., Upton, P.B., Chiang, S.Y., Kow, Y.W., and Swenberg, J.A. (1998). Highly sensitive apurinic/apyrimidinic site assay can detect spontaneous and chemically induced depurination under physiological conditions. Cancer Res. *58*, 222–225.

Nicholls, A., Sharp, K.A., and Honig, B. (1991). Protein folding and association: insights from the interfacial and themodynamic properties of hydrocarbons. Proteins Struct. Funct. Genet. *11*, 281–296.

Ohashi, E., Bebenek, K., Matsuda, T., Feaver, W.J., Gerlach, V.L., Friedberg, E.C., Ohmori, H., and Kunkel, T.A. (2000). Fidelity and processivity of DNA synthesis by DNA polymerase κ, the product of the human DINB1 gene. J. Biol. Chem. *275*, 39678–39684.

Ohmori, H., Friedberg, E.C., Fuchs, R.P., Goodman, M.F., Hanaoka, F., Hinkle, D., Kunkel, T.A., Lawrence, C.W., Livneh, Z., Nohmi, T., et al. (2001). The Y-family of DNA polymerases. Mol. Cell *8*, 7–8.

Otwinowski, Z., and Minor, W. (1997). Processing of X-ray diffraction data collected in oscillation mode. Methods Enzymol. *276*, 307–326.

Parikh, S.S., Putnam, C.D., and Tainer, J.A. (2000). Lessons learned from structural results on uracil-DNA glycosylase. Mutat. Res. *460*, 183–199.

Pelletier, H., Sawaya, M.R., Wolfle, W., Wilson, S.H., and Kraut, J. (1996). Crystal structures of human DNA polymerase β complexed with DNA: implications for catalytic mechanism, processivity, and fidelity. Biochemistry *35*, 12742–12761.

Potapova, O., Grindley, N.D., and Joyce, C.M. (2002). The mutational specificity of the Dbh lesion bypass polymerase and its implications. J. Biol. Chem. *277*, 28157–28166.

Randall, S.K., Eritja, R., Kaplan, B.E., Petruska, J., and Goodman, M.F. (1987). Nucleotide insertion kinetics opposite abasic lesions in DNA. J. Biol. Chem. *262*, 6864–6870.

Rechkoblit, O., Zhang, Y., Guo, D., Wang, Z., Amin, S., Krzeminsky, J., Louneva, N., and Geacintov, N.E. (2002). Trans-lesion synthesis past bulky benzo[*a*]pyrene diol epoxide N2-dG and N6-dA lesions catalyzed by DNA bypass polymerases. J. Biol. Chem. *277*, 30488–30494.

Roberts, R.J., and Cheng, X. (1998). Base flipping. Annu. Rev. Biochem. *67*, 181–198.

Shen, X., Sayer, J.M., Kroth, H., Ponten, I., O'Donnell, M., Woodgate, R., Jerina, D.M., and Goodman, M.F. (2002). Efficiency and accuracy of SOS-induced DNA polymerases replicating benzo[*a*]pyrene-7,8-diol 9,10-epoxide A and G adducts. J. Biol. Chem. *277*, 5265–5274.

Silvian, L.F., Toth, E.A., Pham, P., Goodman, M.F., and Ellenberger, T. (2001). Crystal structure of a DinB family error-prone DNA polymerase from *Sulfolobus solfataricus*. Nat. Struct. Biol. *8*, 984–989.

Strauss, B.S. (1991). The 'A rule' of mutagen specificity: a consequence of DNA polymerase bypass of non-instructional lesions? Bioessays *13*, 79–84.

Suzuki, N., Ohashi, E., Kolbanovskiy, A., Geacintov, N.E., Grollman, A.P., Ohmori, H., and Shibutani, S. (2002). Translesion synthesis by human DNA polymerase κ on a DNA template containing a single stereoisomer of dG-(+)- or dG-(−)-anti-N(2)-BPDE (7,8-dihydroxy-anti-9,10-epoxy-7,8,9,10-tetrahydrobenzo[*a*]pyrene). Biochemistry *41*, 6100–6106.

Tang, M., Pham, P., Shen, X., Taylor, J.S., O'Donnell, M., Woodgate, R., and Goodman, M.F. (2000). Roles of *E. coli* DNA polymerases IV and V in lesion-targeted and untargeted SOS mutagenesis. Nature *404*, 1014–1018.

Trincao, J., Johnson, R.E., Escalante, C.R., Prakash, S., Prakash, L., and Aggarwal, A.K. (2001). Structure of the catalytic core of *S. cerevisiae* DNA polymerase η: implications for translesion DNA synthesis. Mol. Cell *8*, 417–426.

Wagner, J., Gruz, P., Kim, S.R., Yamada, M., Matsui, K., Fuchs, R.P., and Nohmi, T. (1999). The dinB gene encodes a novel *E. coli* DNA polymerase, DNA Pol IV, involved in mutagenesis. Mol. Cell *4*, 281–286.

Wong, I., Patel, S.S., and Johnson, K.A. (1991). An induced-fit kinetic mechanism for DNA replication fidelity: direct measurement by single-turnover kinetics. Biochemistry *30*, 526–537.

Woodgate, R. (1999). A plethora of lesion-replicating DNA polymerases. Genes Dev. *13*, 2191–2195.

Zhang, Y., Yuan, F., Wu, X., Wang, M., Rechkoblit, O., Taylor, J.S., Geacintov, N.E., and Wang, Z. (2000). Error-free and error-prone lesion bypass by human DNA polymerase κ in vitro. Nucleic Acids Res. *28*, 4138–4146.

Zhou, B.L., Pata, J.D., and Steitz, T.A. (2001). Crystal structure of a DinB lesion bypass DNA polymerase catalytic fragment reveals a classic polymerase catalytic domain. Mol. Cell *8*, 427–437.

Accession Numbers

Coordinates reported in this paper have been deposited in the Protein Data Bank with ID codes of 1S0N for Ab-1, 1S0O for Ab-2, 1S10 for Ab-3, 1N56 for Ab-4, and 1N48 for Ab-5.